BMI-1638
(EURAEC 760)

RADIATION STABILITY OF UN URANIUM MONONITRIDE

JOINT U.S.-EURATOM
RESEARCH AND DEVELOPMENT PROGRAM

BATTELLE MEMORIAL INSTITUTE

Printed in USA
Price 75 **cents**

Available from the
Office of Technical Services
U. S. Department of Commerce
Washington 25, D. C.

Report No. BMI-1638
(EURAEC 760)

UC-25 Metals, Ceramics,
and Materials
(TID-4500, 22nd Ed.)

Joint U. S.-Euratom
Research and Development Program

AEC Contract W-7405-eng-92

RADIATION STABILITY OF URANIUM MONONITRIDE

by

Richard A. Wullaert
John F. Lagedrost
Josef Bugl
John E. Gates

June 28, 1963

BATTELLE MEMORIAL INSTITUTE
505 King Avenue
Columbus 1, Ohio

TABLE OF CONTENTS

	Page
ABSTRACT	1
INTRODUCTION	1
EXPERIMENTAL PROCEDURE AND RESULTS	3
Specimen Preparation and Characterization	3
Capsule Design and Dosimentry	6
Corrosion Studies	11
Irradiation History	12
POSTIRRADIATION EXAMINATION AND RESULTS	12
Capsule Opening and Specimen Recovery	13
Gas Sampling	13
Burnup and Dosimetry	16
Dimensional and Density Measurements	16
Metallography	19
Microhardness	28
DISCUSSION OF RESULTS	28
CONCLUSIONS	32
REFERENCES	32

EXPERIMENTAL PROCEDURE AND RESULTS

The purpose of this investigation was to study the radiation stability of uranium mononitride. Specifically, any detrimental effects produced in UN by the fissioning of uranium or by the $N^{14}(n,p)C^{14}$ reaction were to be determined. The experimental variables were chosen to enable a semiquantitative evaluation of the effects of hydrogen accumulation from the (n,p) reaction. This was accomplished by irradiating UN specimens with the same uranium content, but with different U^{235} enrichments, in similar neutron fluxes. The amount of hydrogen produced by the (n,p) reaction was a function only of the integrated neutron flux, while the amount of fission gas produced was a function of both the uranium enrichment and the integrated neutron flux, as shown in Figure 1. Thus, to a certain degree, this enabled the effects of hydrogen to be separated from the effects of fission gas. The irradiation temperatures were minimized for this aspect of the investigation in order to maximize the retention of hydrogen.

Specimens of UN fabricated from depleted, natural, and enriched uranium, and contained in six noninstrumented capsules (BMI-40-1 through BMI-40-6) were irradiated in the Materials Testing Reactor for approximately 6 months in thermal-neutron fluxes of around 1×10^{14} nv. Each capsule was made of thick-walled aluminum and contained two UN specimens of the same enrichment. One of the specimens was in direct contact with the NaK used as the heat-transfer medium in the capsule, while the other was enclosed in stainless steel cladding. An exception was Capsule BMI-40-6, which contained three specimens: one clad, one partially clad (no end caps), and one unclad. The post-irradiation evaluation of the specimens included determination of dimensional-stability and fission-gas and hydrogen release, metallography, and microhardness measurements.

Specimen Preparation and Characterization

UN powder was prepared by the direct reaction of nibbled uranium metal with prepurified nitrogen.[1] The reaction product, a higher nitride with a nitrogen/uranium ratio above 1.5, was subsequently decomposed to UN in vacuum at 1300 C. Some of the irradiation specimens were fabricated with a Carbowax 6000 binder and some without binder. Green pellets with densities of 70 to 75 per cent of theoretical were formed at a pressure of 80,000 to 100,000 psi in steel dies. The precompacted pellets were hot pressed to densities up to 99 per cent of theoretical by means of isostatic hot pressing. The pellets were sealed in niobium cans and hot pressed at 1480 C for 3 hr under a 10,000-psi gas pressure. The irradiation specimens were obtained by grinding off the niobium cladding and the slight reaction zone between niobium and UN with a diamond wheel. Typical specimens are shown in Figure 2. A number of specimens were slip-fitted into 15-mil Type 304 stainless steel claddings, and the end caps were sealed by a Heliarc weld. Figure 3 is a photograph of typical clad UN specimens. Some of these clad specimens were pressure bonded at 1150 C to remove the core-cladding gap. The bonding achieved is shown in Figure 4.

(1)References at end.

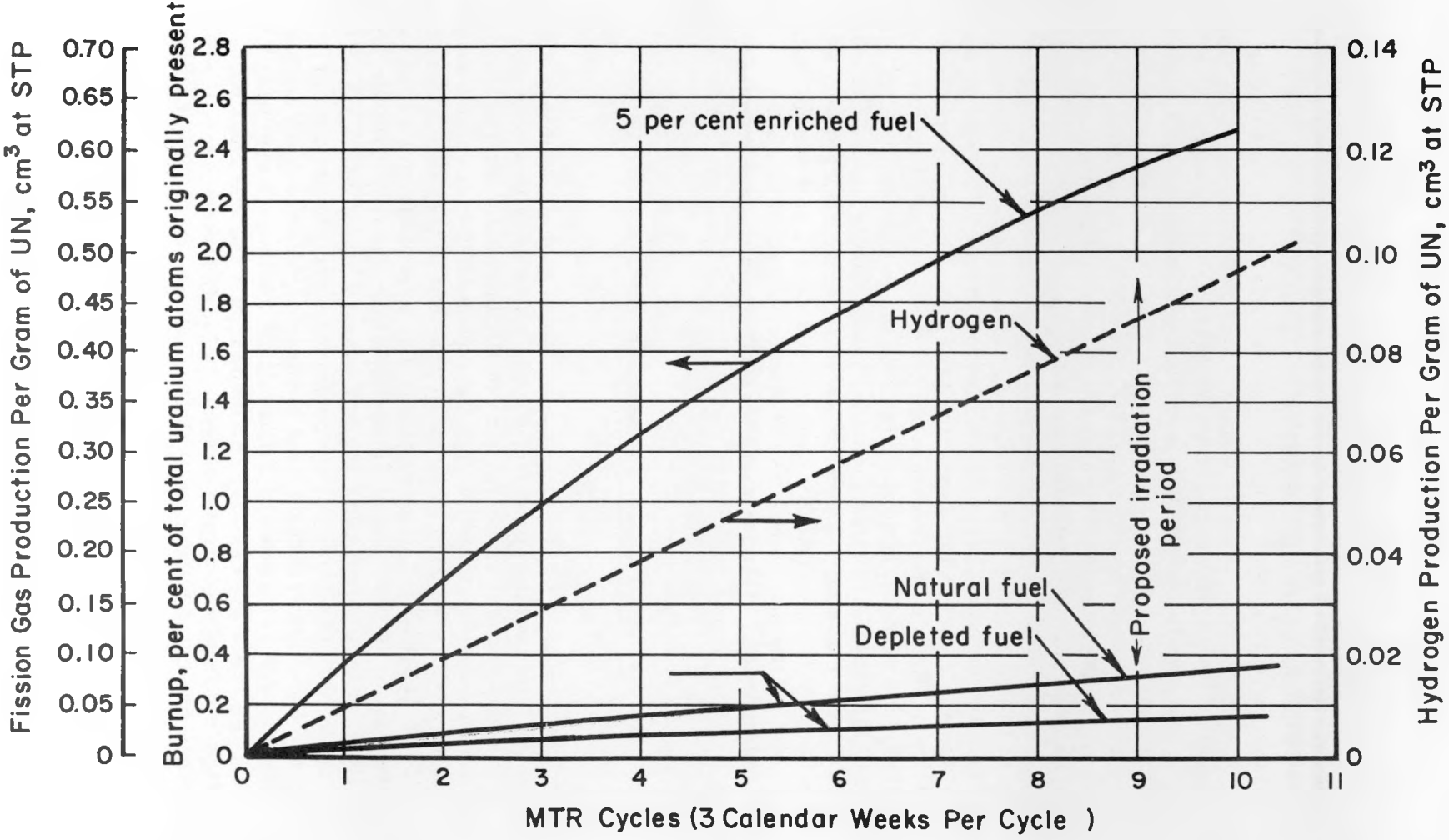

FIGURE 1. ESTIMATED FISSION-GAS, URANIUM-BURNUP, AND HYDROGEN-PRODUCTION RATES IN UN SPECIMENS BASED ON A SPECIMEN-EFFECTIVE THERMAL-NEUTRON FLUX OF 1 X 10^{14} Nv

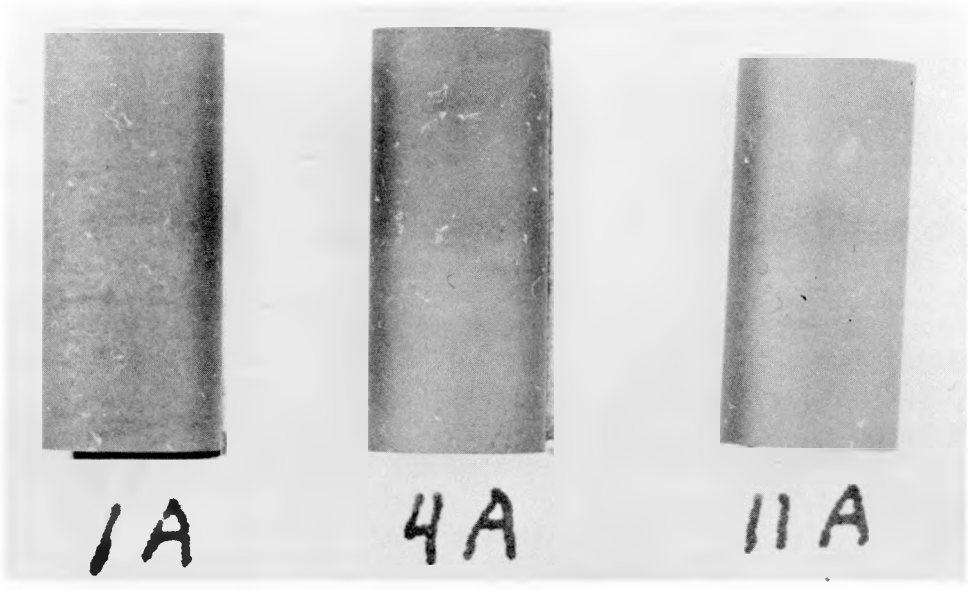

3X RM18597

FIGURE 2. TYPICAL APPEARANCE OF URANIUM MONONITRIDE SPECIMENS BEFORE IRRADIATION

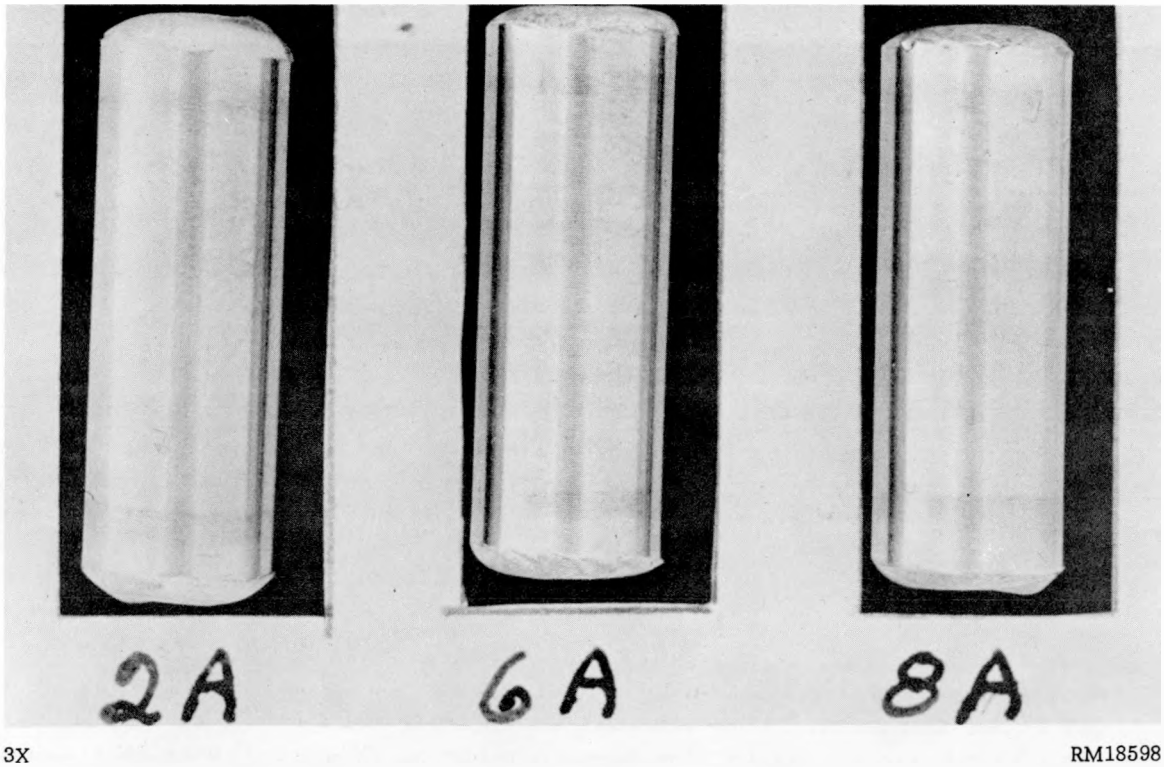

3X RM18598

FIGURE 3. TYPICAL APPEARANCE OF STAINLESS STEEL CLAD URANIUM MONONITRIDE SPECIMENS BEFORE IRRADIATION

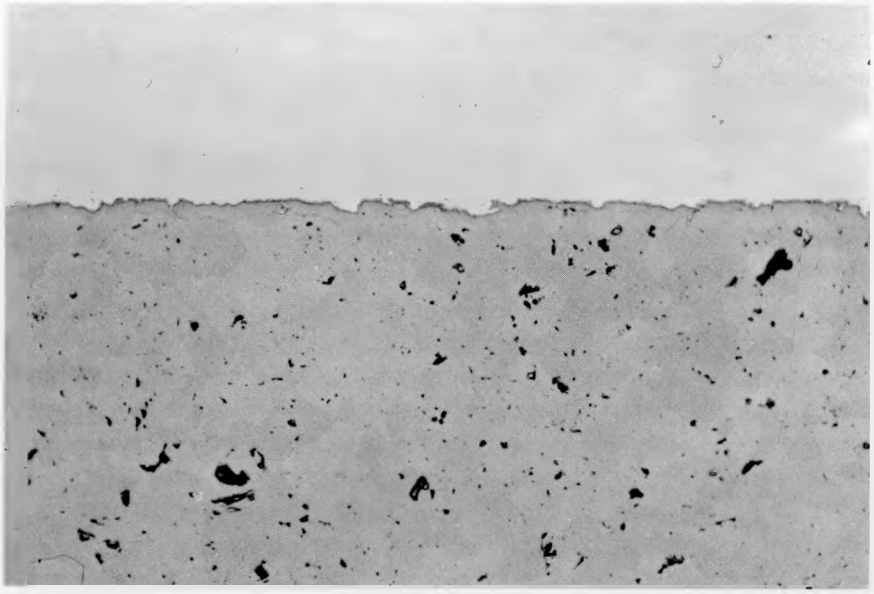

250X N80942

FIGURE 4. CORE-CLADDING INTERFACE IN TYPICAL TYPE 304 STAINLESS STEEL-CLAD UN IRRADIATION SPECIMEN

The UN specimens fabricated with Carbowax 6000 had more visible impurity phases than the specimens fabricated without the use of a binder. Figure 5 shows typical microstructures of UN fabricated with a binder and without a binder. The differences were a greater porosity and larger quantities of a second phase in specimens made with a binder. The second phase has been identified as a mixture of UO_2 and a higher uranium nitride.[1]

Chemical analyses, vacuum-fusion analyses, and X-ray analyses were performed on control specimens of UN. The preirradiation density of the fuel pellets was also measured. Results are given in Table 2.

Capsule Design and Dosimetry

The primary consideration in the capsule design was the requirement that the irradiations be conducted at a minimum temperature to enhance the retention of hydrogen within the UN. Therefore, only materials having high thermal conductivities were used for capsule construction. Figure 6 shows an assembly drawing of the capsule and Figure 7 is a photograph of the capsule components ready for assembly.

The capsule body and headers were fabricated from Type 6061-T6 aluminum. The capsule-wall thickness was a maximum to utilize as much as possible the high thermal conductivity of the aluminum. The nominal dimensions were 1-1/8 in. in OD by 0.390 in. in ID by 4-1/2 in. long. The specimen basket (Figure 7) was fabricated from nickel-cobalt dosimeter wire, and suspended the specimens in NaK. Aluminum-cobalt dosimeter wires were positioned on the outside surface of the capsule, as shown in Figure 6. These wires were periodically removed and analyzed during the capsule irradiation to provide estimates of specimen temperature and burnup as the irradiation progressed.

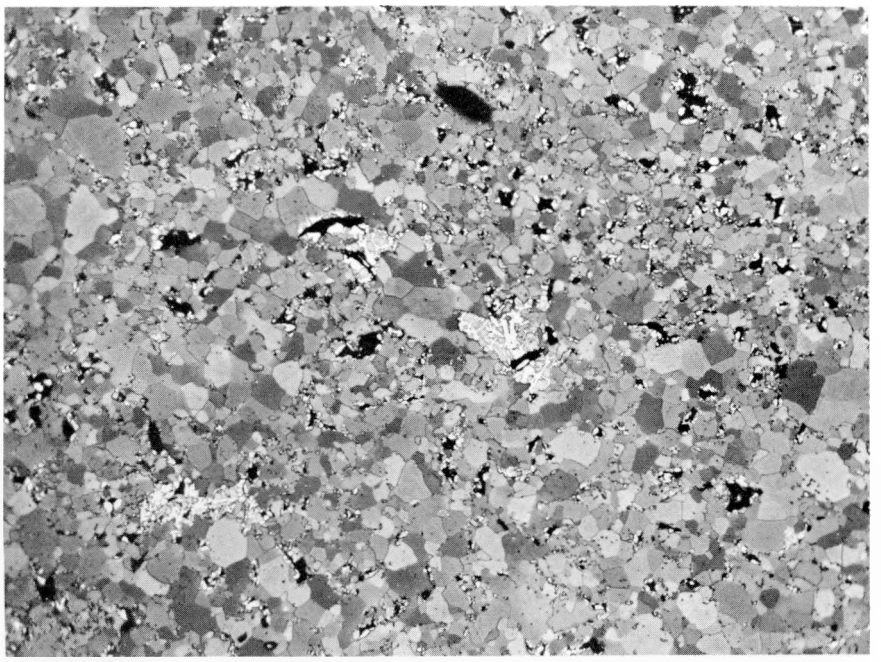

250X RM21181

a. Carbowax 6000 Binder

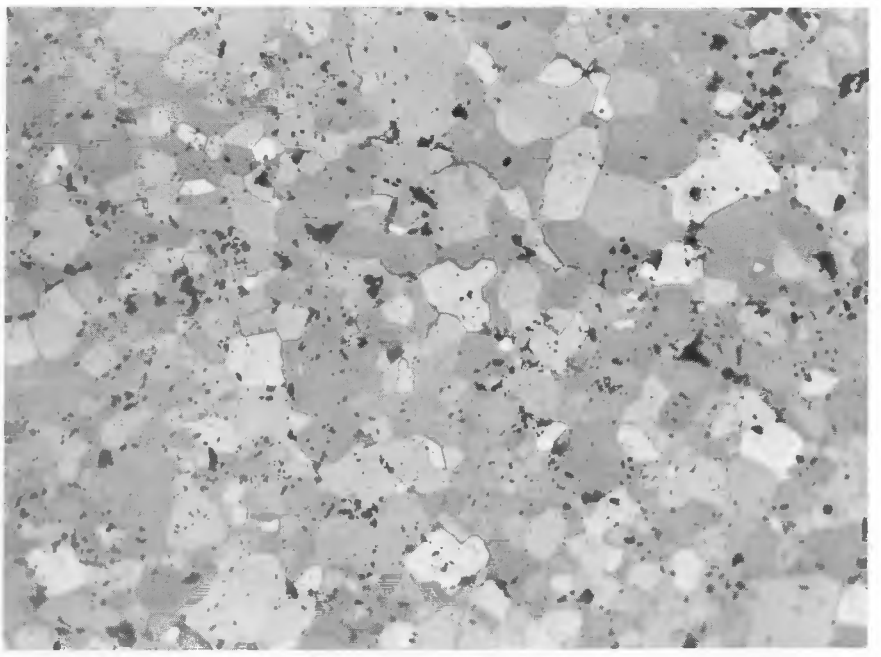

250X RM21194

b. No Binder

FIGURE 5. EFFECT OF USE OF A BINDER DURING FABRICATION ON THE MICROSTRUCTURE OF UN IRRADIATION SPECIMENS

Note second phase, probably UO_2 and a higher uranium nitride, in the specimen prepared with a binder. Etched nonirradiated specimens are shown.

TABLE 2. COMPOSITION OF IRRADIATION SPECIMENS

Capsule	Specimen	Uranium Enrichment, per cent	Density		Lattice Constant, A	Uranium, w/o	Nitrogen, w/o	Carbon, w/o	Oxygen, ppm	Hydrogen, ppm
			G per Cm^3	Per Cent of Theoretical						
BMI-40-1	4A	0.224	13.73	95.9	4.8903	---	--	--	1660	3
	6A	0.224	13.73	95.9	--	---	5.42	0.024	--	--
BMI-40-2	15	0.224	13.92	97.2	4.8889	94.35	5.53	0.008	580	4
	13	0.224	13.87	96.9	4.8878	94.31	5.48	0.009	540	6
BMI-40-3	1A	0.72	13.65	95.3	4.8888	--	5.30	0.04	1250	2
	2A	0.72	13.61	95.0	--	--	5.39	0.06	2730	11
BMI-40-4	19	0.72	13.87	96.9	4.8888	94.28	5.54	0.037	490	2
	17	0.72	13.73	95.9	4.8891	94.61	5.45	0.027	520	2
BMI-40-5	11A	5.08	13.65	95.3	--	--	--	--	--	--
	8A	5.08	13.77	96.2	4.8894	--	5.43	0.042	1480	3
BMI-40-6	23	5.08	14.20	99.1	4.8884	94.47	5.52	0.012	740	<1
	21	5.08	14.19	99.0	4.8883	94.56	5.40	0.016	820	<1
	9A[a]	5.08	14.20	99.1	4.8894	--	5.43	0.042	1480	3
	22[a]	5.08	14.20	99.1	4.8884	94.47	5.52	0.012	740	<1

(a) Pellets 9A and 22 were contained in a single clad specimen designated 9A-22.

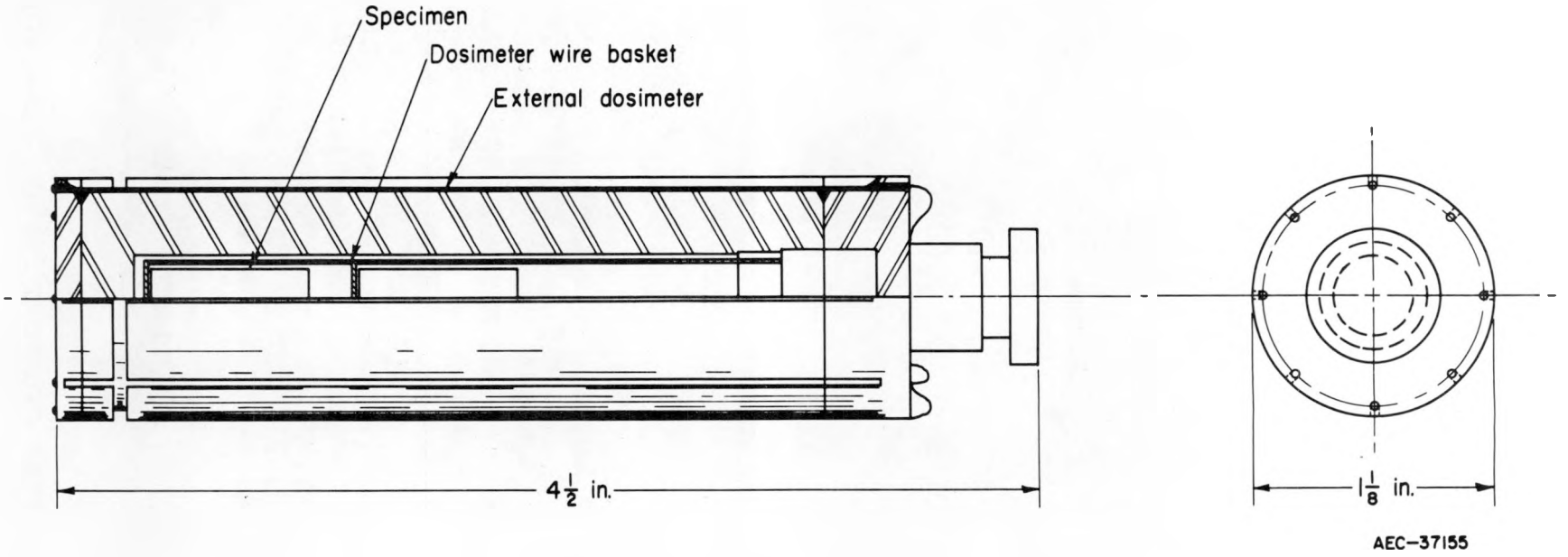

FIGURE 6. CAPSULE FOR URANIUM MONONITRIDE IRRADIATIONS

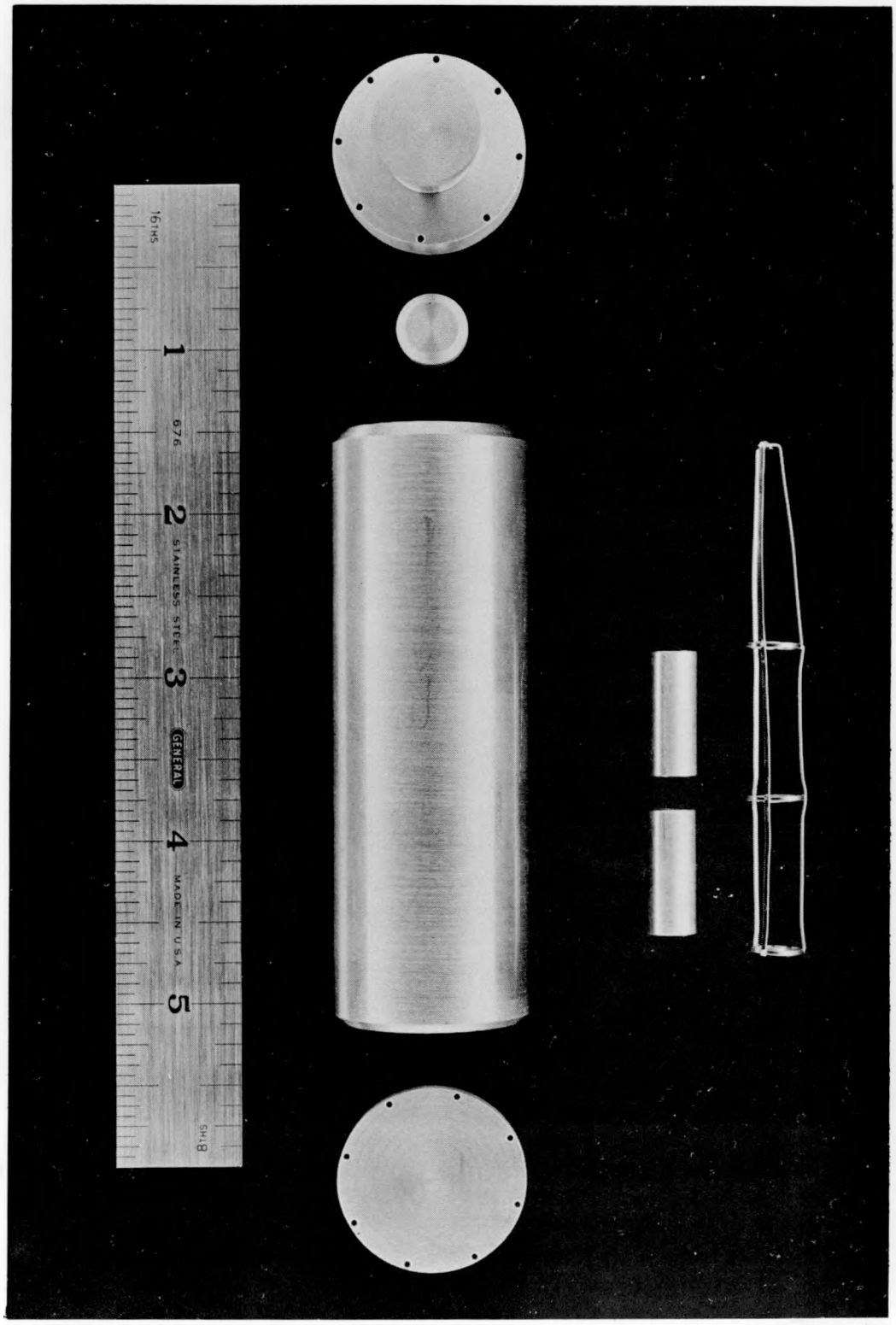

IX N78151

FIGURE 7. CAPSULE COMPONENTS AND FUEL SPECIMENS PRIOR TO ASSEMBLY

Estimates of the temperatures generated at the fuel surface and fuel center line by an effective thermal-neutron flux of 1×10^{14} nv were made by standard calculation methods. Results of a computer program set up to study the heat-generation and heat-transfer conditions in the capsule substantiated these estimates. Furthermore, it was found that the surface temperatures would be quite uniform over a large fraction of the length of each specimen, even though opportunity existed for nonradial heat flow in the aluminum containment wall. This finding reduced the concern about nonradial heat-flow effects which, if significant, would have complicated severely the problem of estimating the specimen-temperature profile during irradiation. The final capsule design criteria are given in Table 3.

TABLE 3. CAPSULE DESIGN CRITERIA

Capsule	Specimen Enrichment, per cent	Specimen-Effective Thermal-Neutron Flux, 10^{14} nv	Total Uranium Burnup, per cent	Specimen-Surface Temperature, C
BMI-40-1	0.224	1.0	0.14	75
BMI-40-2	0.224	1.0	0.14	75
BMI-40-3	0.72	1.0	0.33	105
BMI-40-4	0.72	1.0	0.33	105
BMI-40-5	5.08	0.5	1.4	230
BMI-40-6	5.08	1.0	2.3	390

Corrosion Studies

Within the capsules, aluminum, nickel, stainless steel, and uranium mononitride were in contact with NaK. Stainless steel and nickel have good resistance to NaK corrosion at temperatures above those anticipated in this irradiation program.[2] Aluminum in low-alloy forms resists alkaline-metal attack at temperatures up to 250 C.[2]

Since information on the attack of NaK on UN was not available, two NaK-UN-aluminum compatibility experiments were conducted. The tests were conducted at 260 C for 1000 hr and at 480 C for 1500 hr. Two UN samples, 1/2 in. in OD by 1/2 in. long, were placed in aluminum baskets and immersed in NaK-56 in sealed stainless steel capsules. No UN corrosion was evident at the conclusion of the experiments, although there was a 0.2 per cent weight gain in the UN. A slight amount of aluminum was found in the residue from the reacted NaK after the 480 C experiment; at this temperature, some NaK-aluminum attack would be expected. No evidence of aluminum corrosion was found in the 260 C capsule. Since the peak estimated aluminum-NaK interface temperature in the capsules was 260 C, it was believed that corrosion in the irradiation capsules would not be a problem.

Irradiation History

Capsules BMI-40-1 through BMI-40-6 were inserted in the MTR, and as the irradiations progressed dosimeter wires were removed from the outer surfaces of the capsules. These dosimeters were analyzed to determine the capsule-surface thermal-neutron flux. These data were translated to specimen-effective flux by use of capsule flux profiles provided by IBM-650 calculation with the P-3 code.[3] It was concluded from these data that the irradiations of Capsules BMI-40-1 through BMI-40-5 were progressing satisfactorily, although, in most cases, the flux levels appeared to be higher than the design targets.

The initial specimen-effective flux in Capsule BMI-40-6, estimated from dosimetry, was approximately twice the design condition. In this case, the specimen-surface temperature was probably higher than 540 C and the inner wall temperature of the aluminum may have exceeded 260 C. This fostered a concern that some degree of incompatibility between NaK and aluminum might occur and that the resultant specimen damage might be more severe than that from normal radiation effects. Subsequently, the capsule was relocated to a lower flux in the same reactor facility to obtain a general reduction of temperature level. The in-pile history is summarized in Table 4.

TABLE 4. IN-PILE HISTORY FOR THE BMI-40 CAPSULE SERIES

Capsule	MTR Position	Reactor-Quoted Unperturbed Thermal-Neutron Flux, 10^{14} nv	Average Flux Level at Capsule Surface From Dosimetry(a), 10^{14} nv	Irradiation Time, days
BMI-40-1	A-38-NE	1.5	1.3	101
	A-38-NW	1.6	--	44
BMI-40-2	L-52-NE	1.9	1.7	148
BMI-40-3	A-38-NE	1.5	1.4	101
	L-52-SW	1.6	--	40
BMI-40-4	L-52-SW	1.7	1.0	138
BMI-40-5	A-39-SW	1.4	1.1	145
BMI-40-6	L-58-C	3.3	2.6	68
		2.8	--	80

(a) The specimen-effective flux is given later in Table 7.

POSTIRRADIATION EXAMINATION AND RESULTS

After discharge from the MTR, the capsules were returned to the Battelle Hot-Cell Facility where they were disassembled and the specimens recovered for examination. The postirradiation examination of the specimens consisted of visual examinations of the capsules and specimens, sampling and analysis of the gas contained in one capsule

and a clad specimen from the same capsule, dosimeter-wire and specimen-burnup analyses, dimensional and density measurements, a study of the microstructure of the fuel and cladding, and microhardness measurements on the fuel.

Capsule Opening and Specimen Recovery

Capsules BMI-40-1 through BMI-40-6 were visually examined, and nothing unusual was noted at magnifications up to 6 diameters. The capsules were opened (the gas content of BMI-40-6 was sampled before opening) and the NaK reacted with butyl alcohol. Immediately upon removal of the specimens from the capsules, it was observed that the unclad specimen in each capsule had broken into several pieces (Figures 8 and 9). By opening a capsule under mineral oil, it was established that the specimens were broken prior to the NaK-butyl alcohol reaction. All of the broken sections appeared solid and not friable. The number of fragments increased and their size decreased as the burnup and temperature increased (compare Figures 8 and 9). Many of the pieces appeared to originally result from concave and convex fractures perpendicular to the axis of the cylindrical specimens (Figure 8).

There was nothing unusual about the appearance of the stainless steel-clad specimens, except some blackening of the surface of the cladding on the clad specimen from Capsule BMI-40-6. There did not appear to be any noticeable corrosion of the aluminum interior of Capsule BMI-40-6.

Gas Sampling

Capsule BMI-40-6, which contained specimens subjected to the most severe temperature and burnup conditions, was selected for gas sampling. The gas content inside the capsule was collected by drilling a hole through the bottom of the capsule. The entire drilling operation was conducted in an evacuated chamber, and the released gas was pumped into vials of known volume by means of a Toepler pump. The collected gas was analyzed by mass and gamma-ray spectrometry to determine the fission-gas and hydrogen content. The results are listed in Tables 5 and 6.

Analyses for krypton and xenon indicated that about 0.3 to 0.6 per cent of the fission gases produced in the UN was released. The amount of hydrogen produced in the UN during the irradiation was calculated to be 14.8 ppm, using an integrated thermal-neutron flux of 2.0×10^{20} nvt and a cross section of 1.75 mb for the $N^{14}(n,p)C^{14}$ reaction.[4] If it is assumed that the hydrogen found in the capsule was released from the unclad and the partially clad specimens (21 and 23), then about 35 per cent of the hydrogen produced in the UN was released to the capsule. Analysis of the fully clad specimen (9A-22) in the same capsule showed that only 2.6 per cent of the hydrogen produced in the UN was found contained within the stainless steel can. This may indicate that hydrogen escaped through the cladding to the capsule. If this was the case, then about 26 per cent of the hydrogen produced in the UN in Capsule BMI-40-6 was released into the capsule.

4X HC9245

FIGURE 8. UN IRRADIATED AT A MAXIMUM CENTER-LINE TEMPERATURE OF 200 C TO AN URANIUM BURNUP OF 0.34 a/o (SPECIMEN 19 FROM CAPSULE BMI-40-4)

4X HC8848

FIGURE 9. UN IRRADIATED AT A MAXIMUM CENTER-LINE TEMPERATURE OF 650 C TO AN URANIUM BURNUP OF 2.1 a/o (SPECIMEN 11A FROM CAPSULE BMI-40-5)

TABLE 5. FISSION-GAS-RELEASE DATA FOR URANIUM MONONITRIDE IRRADIATED IN CAPSULE BMI-40-6[a]

Source	Gas	Gas Produced, 10^{19} atoms	Gas Released, 10^{17} atoms	$\frac{\text{Gas Released}}{\text{Gas Produced}} \times 100$
		Mass-Spectrometry Data		
Capsule[b]	Xe^{131}	4.95	1.72	0.35
	Xe^{132}	7.50	3.69	0.49
	Xe^{134}	13.0	5.91	0.46
	Xe^{136}	20.8	9.17	0.45
Clad specimen (9A-22)	Xe^{131}	1.92	0.74	0.39
	Xe^{132}	2.91	1.54	0.53
	Xe^{134}	5.04	2.54	0.51
	Xe^{136}	8.06	3.93	0.48
Capsule[b]	Kr^{83}	0.82	0.33	0.40
	Kr^{84}	1.87	1.08	0.58
	Kr^{85}	0.51	0.26	0.51
	Kr^{86}	3.58	1.75	0.49
Clad specimen (9A-22)	Kr^{83}	0.31	0.14	0.44
	Kr^{84}	0.73	0.43	0.59
	Kr^{85}	0.20	0.10	0.51
	Kr^{86}	1.39	0.68	0.48
		Gamma Spectroscopy		
Capsule[b]	Kr^{85}	0.51	0.28	0.56
Clad specimen (9A-22)	Kr^{85}	0.20	0.08	0.38

(a) U^{235} enrichment = 5.08 per cent. Maximum Temperature: Surface, 615 C
Total uranium burnup = 3.8 per cent. Center line, 1260 C.
(b) Source of fission gases assumed to be unclad and partially clad specimens.

TABLE 6. HYDROGEN-GAS-RELEASE DATA FOR UN IRRADIATED IN CAPSULE BMI-40-6[a]

Source	Gas Produced			Volume of Gas Released, cm^3	$\frac{\text{Gas Released}}{\text{Gas Produced}} \times 100$
	Weight, ppm	Volume, cm^3 Per G of UN	Volume, cm^3 Total		
Capsule[b]	14.8	0.17	3.4	1.18	35
Clad specimen (9A-22)	14.8	0.17	1.3	0.03	2.6

(a) U^{235} enrichment = 5.08 per cent. Maximum temperature: Surface, 615 C
Total uranium burnup = 3.8 per cent. Center line, 1260 C.
(b) Source of hydrogen assumed to be unclad and partially clad specimens.

Burnup and Dosimetry

Postirradiation examination included analyses of capsule-surface dosimeter wires to determine full-term integrated-flux levels, and isotopic burnup analyses of representative sections of specimens from Capsules BMI-40-3, BMI-40-5, and BMI-40-6. A summary of these determinations is presented in Table 7. For cases where isotopic burnup data were not available, the specimen-effective fluxes were estimated on the basis of the surface-dosimeter data. Generally, the latter are in agreement with corresponding dosimeter data obtained during the early stages of the irradiations.

Estimated specimen temperatures are also presented in Table 7. These were calculated from:

(1) Fission heat-generation rates obtained on the basis of the burnup estimates

(2) Gamma heating rates reported for the reactor facilities

(3) The capsule-design heat-transfer analyses.

In arriving at the temperature estimates, consideration was given to the fact that as the high fuel-burnup levels were reached, perturbation of the neutron flux by the specimens decreased somewhat. Thus, the fission heat-generation rates, and consequently the capsule temperatures, did not decrease in direct proportion to the burnup levels, but decreased at somewhat lower rates. For example, it is estimated in the case of Capsule BMI-40-5 that the temperature decrease from start to termination of irradiation was only about 60 C (specimen surface) even though nearly half of the fuel was burned up at termination.

The production of Pu^{239} from absorption of neutrons in U^{238}, and the subsequent fissioning of the Pu^{239}, were also examined to obtain nuclear heat-production rates for the temperature-estimating procedures. The plutonium contribution was found to be approximately 30 per cent of the total fission heat generated at the end of the irradiations of the depleted and natural uranium specimens, and 10 to 20 per cent in the specimens of slightly enriched fuel.

Dimensional and Density Measurements

The physical dimensions and density of the specimens were measured before and after irradiation. Because of the breakup of the unclad specimens, only the diameter and density of a few specimens were obtained. Dimensions were measured with standard friction-thimble micrometers to at least ±0.0005 in. Densities were measured by standard immersion techniques in carbon tetrachloride at 25 C to at least ±0.03 g per cm^3. The data are presented in Table 8.

The diametrical changes along the length of the specimens were uniform, except for the partially clad (Specimen 21) and the fully clad (9A-22) specimen irradiated in Capsule BMI-40-6. The partially clad specimen swelled more at both ends and exhibited a measured increase in diameter of 2.4 per cent at the ends compared to 1.3 per cent at

TABLE 7. DOSIMETRY, BURNUP, AND IRRADIATION-TEMPERATURE DATA FOR UN

Capsule	Burnup		Average Specimen-Effective Flux, 10^{14} nv	Total Integrated Effective Flux, 10^{21} nvt	Initial Heat-Generation Rate, 10^4 Btu/(hr)(ft^2)	Specimen Temperature[a], C			
	Per Cent of Total Uranium	10^{20} Fissions Per Cm^3 of UN				Surface		Center Line	
						Start	End	Start	End
BMI-40-1	0.13[b]	0.43	1.0	1.3	7.2	70	65	120	105
BMI-40-2	0.16[b]	0.53	1.4	1.8	9.6	75	65	140	100
BMI-40-3	0.43[c]	1.4	1.0	1.2	23.2	110	90	240	190
BMI-40-4	0.34[b]	1.1	0.75	0.9	17.1	100	90	200	170
BMI-40-5	2.10[c]	6.9	0.64	0.8	90.4	280	220	650	500
BMI-40-6	3.80[c]	13	1.5	1.9	244	615	255	1260	575

(a) Specimen-temperature gradients computed on the basis of uniform heat generation and the following values of thermal conductivity for UN: 0.03 cal/sec-cm-°C at 200 C and 0.06 cal/sec-cm-°C at 1000 C. The thermal conductivity was assumed to be approximately linear between these temperatures.

(b) Values estimated from isotopic analysis and dosimetry data.

(c) Values obtained from isotopic analysis.

TABLE 8. DIMENSION AND DENSITY CHANGES IN IRRADIATED UN

Capsule	Specimen[a]	Diameter			Length			Density		
		Preirradiation, in.	Postirradiation, in.	Change, per cent	Preirradiation, in.	Postirradiation, in.	Change, per cent	Preirradiation, g per cm^3	Postirradiation[b], g per cm^3	Change, per cent
BMI-40-1	4A	0.3002	0.3016	0.47	0.7207	--	--	13.73	13.63	-0.73
	6A(SF)	0.3306	0.3312	0.18	0.9918	0.9945	0.27	11.45	11.47	0
	6A*	0.3007	0.3021	0.47	0.7114	0.7150	0.51	13.73	13.51	-1.6
BMI-40-2	15	0.3003	0.3024	0.70	0.7508	--	--	13.92	13.46	-3.3
	13(PB)	0.3290	0.3291	0.73	1.0093	1.0174	0.80	11.67	11.55	-1.0
BMI-40-3	1A	0.2998	--	--	0.7112	--	--	13.65	13.50	-1.1
	2A(SF)	0.3303	0.3311	0.24	1.033	1.0315	0.10	11.32	11.35	0
	2A*	0.3005	0.3019	0.47	0.7308	0.7369	0.83	13.61	13.38	-1.7
BMI-40-4	19	0.3003	0.3028	0.83	0.7506	--	--	13.87	13.51	-2.6
	17(PB)	0.3300	0.3305	0.15	1.0017	1.0099	0.81	11.68	11.54	-1.2
BMI-40-5	11A	0.3006	--	--	0.6611	--	--	13.65	13.26	-2.9
	8A(SF)	0.3303	0.3321	0.55	0.9854	0.9873	0.19	11.45	11.38	-0.61
	8A*	0.3007	0.3040	1.10	0.6949	0.7000	0.73	13.77	13.36	-3.0
BMI-40-6	23	0.3000	--	--	0.7494	--	--	14.20	--	--
	21(PB)[c]	0.3284	0.3343	1.76[d]	0.5134	0.5250	2.26	14.19	--	-6.4[e]
	9A-22(PB)[f]	0.3292	0.3337	1.35[d]	0.7714	0.7758	0.57	--	--	-3.5[e]

(a) "A" denotes specimens fabricated with a binder, (SF) denotes slip-fitted cladding, (PB) denotes pressure bonded cladding, * denotes slip-fitted specimens which were declad.
(b) Estimated accuracy of postirradiation density measurement is ±0.03 g per cm^3.
(c) Specimen ends were not clad.
(d) Average of nonuniform change.
(e) Volume increase based on dimensional measurements.
(f) Fully clad specimen contained two UN pellets.

the middle. It should be noted that the ends of the specimen were exposed to NaK during the irradiation. The fully clad specimen exhibited a diametrical increase of 1.6 per cent at the middle and 1.2 per cent at the ends.

The UN pellets which had slip-fitted cladding were removed from their cladding without any damage to the fuel. All of the pellets (6A, 2A, and 8A) were observed to be in excellent condition (Figure 10). The remaining clad specimens were clad by pressure-bonding techniques, bonding the cladding to the core and making it impossible to recover the fuel pellets without damage.

In handling the pellets from which the cladding had been removed, two of them (6A and 2A) fractured by mechanical shock. The type of fracture and the appearance of the fracture surface are shown in Figure 11.

Metallography

Longitudinal and transverse sections from eight representative specimens were selected for metallographic examination. The transverse sections were mounted in Bakelite, and the longitudinal sections were mounted in Hysol plastic. The specimens were ground through 240-, 400-, and 600-grit SiC paper using water as a lubricant. Polishing was accomplished on Microcloth using a Linde B and 2 per cent CrO_3 abrasive water slurry. The final polish was done on Microcloth using just Linde B abrasive in water. The specimens were examined at magnifications up to 1000X in the as-polished condition and after swab etching. The Type 304 stainless steel cladding was etched with 20 cm^3 of glycerin, 20 cm^3 of HCl, and 4 cm^3 of HNO_3. The uranium mononitride was etched with a 60 cm^3 lactic acid- 24 cm^3 HNO_3, -2 cm^3 HF mixture(5).

The microstructure of UN after the low-temperature irradiations (Capsules BMI-40-1 through BMI-40-4) is shown in Figures 12, 13, 14, and 15. Just as in unirradiated UN, the second phase was still associated with pores, and was predominately in the UN made with a wax binder. Comparison of the microstructure of the irradiated UN (Figures 12 through 15) with the microstructure of the unirradiated UN (Figure 5) shows that very little, if any, changes occurred in the UN after irradiation to low burnups at low temperatures.

The microstructure of UN irradiated at somewhat higher temperatures, 650 C at the center line and 280 C at the surface (Capsule BMI-40-5), is shown in the etched condition in Figure 16. Again, very little change was evident in the UN, except for a slight rounding of the pores.

The specimens irradiated in Capsule BMI-40-6 were subjected to the most stringent temperature and burnup conditions (Table 7) of any of the specimens irradiated in this program. Composite views of Pellets 9A and 22 from Specimen 9A-22 are shown in Figures 17 and 18. In the UN made with a binder (9A), a second phase appeared in two forms. In the center of the pellet, the second phase was distributed in the grain boundaries (Figures 17 and 19). Approaching the outer edge of the pellet, the white phase appeared to form in larger quantities (Figure 17), sometimes around and in cracks (Figure 20).

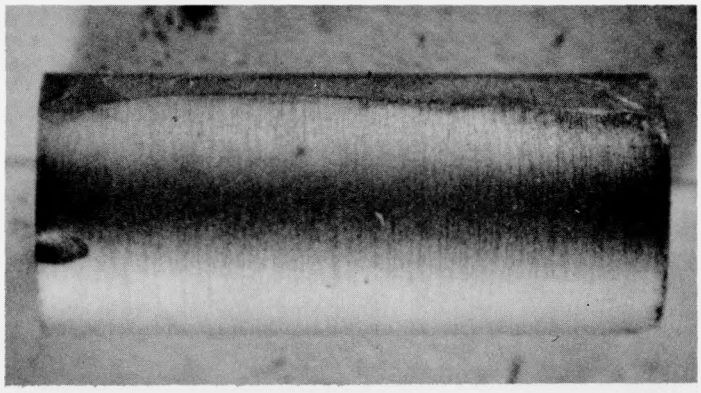

4X HC8861

FIGURE 10. ORIGINALLY CLAD IRRADIATED UN AFTER REMOVAL OF CLADDING

The marks on the fuel are due to abrasion during removal of the cladding (Specimen 8A from Capsule BMI-40-5).

6X HC9246

FIGURE 11. APPEARANCE OF FRACTURE PRODUCED IN IRRADIATED UN BY MECHANICAL SHOCK AFTER REMOVAL OF CLADDING (SPECIMEN 2A FROM CAPSULE BMI-40-3)

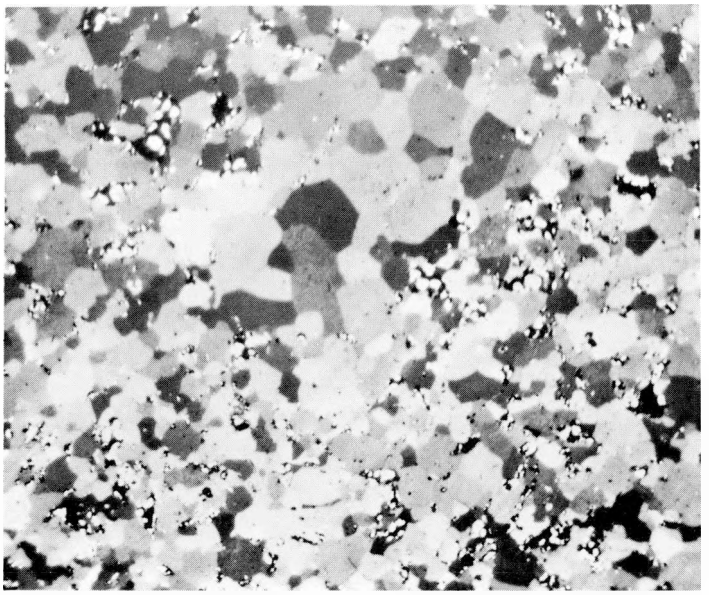

250X HC9390

FIGURE 12. MICROSTRUCTURE OF UN (MADE WITH WAX BINDER) IRRADIATED TO AN URANIUM BURNUP OF 0.13 a/o AT A MAXIMUM CENTER-LINE TEMPERATURE OF 120 C (SPECIMEN 4A FROM CAPSULE BMI-40-1)

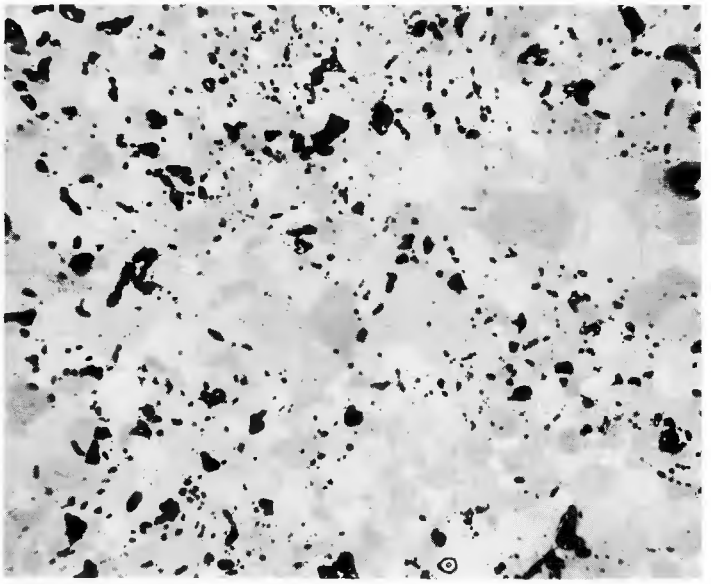

250X HC9410

FIGURE 13. MICROSTRUCTURE OF UN (NO BINDER) IRRADIATED TO AN URANIUM BURNUP OF 0.16 a/o AT A MAXIMUM CENTER-LINE TEMPERATURE OF 140 C (SPECIMEN 13 FROM CAPSULE BMI-40-2)

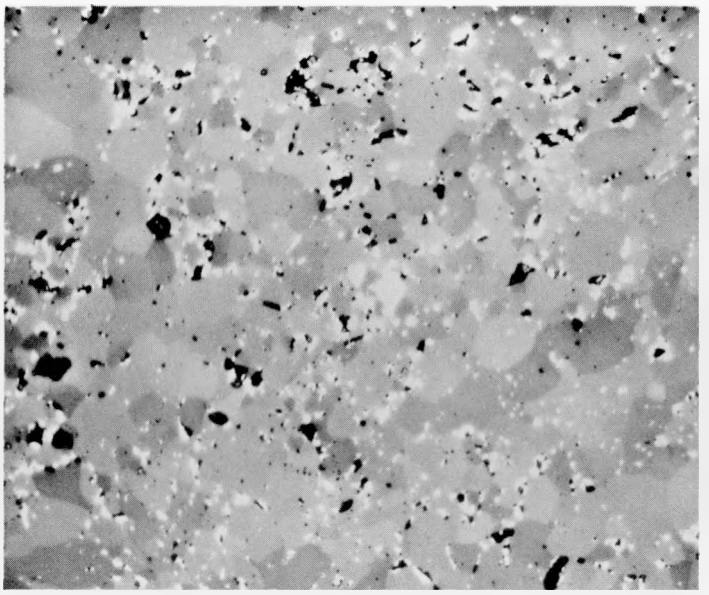

250X HC9388

FIGURE 14. MICROSTRUCTURE OF UN (MADE WITH WAX BINDER) IRRADIATED TO AN URANIUM BURNUP OF 0.43 w/o AT A MAXIMUM CENTER-LINE TEMPERATURE OF 240 C (SPECIMEN 1A FROM CAPSULE BMI-40-3)

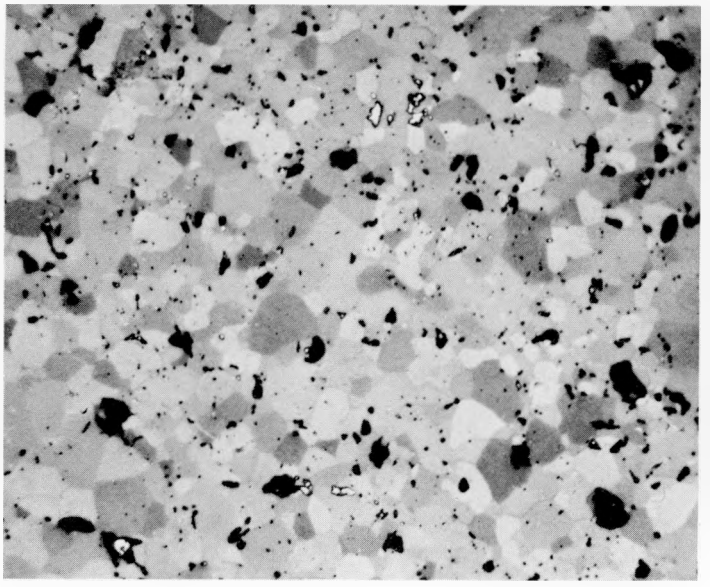

250X HC9422

FIGURE 15. MICROSTRUCTURE OF UN (NO BINDER) IRRADIATED TO AN URANIUM BURNUP OF 0.34 a/o AT A MAXIMUM CENTER-LINE TEMPERATURE OF 200 C (SPECIMEN 17 FROM CAPSULE BMI-40-4)

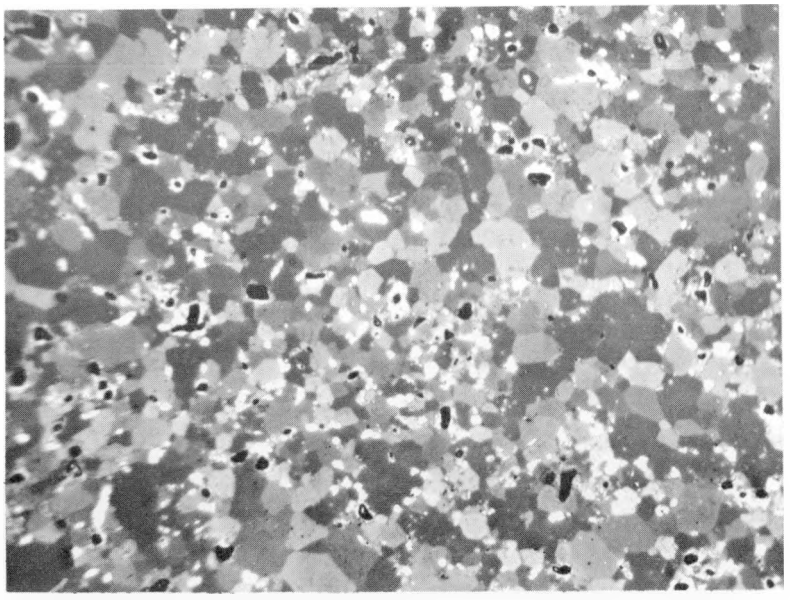

250X HC9393

FIGURE 16. MICROSTRUCTURE OF UN (MADE WITH WAX BINDER) AFTER IRRADIATION TO A URANIUM BURNUP OF 2.1 a/o AT A MAXIMUM CENTER-LINE TEMPERATURE OF 650 C (SPECIMEN 8A FROM CAPSULE BMI-40-5)

The other pellet examined from Capsule BMI-40-6 (Pellet 22) was not fabricated with a binder and the second phase only appeared near the UN-cladding interface (Figure 18). In both pellets (9A and 22), the second phase appeared to have precipitated at the UN-cladding interface to a depth of about 0.030 in. into the fuel, and mainly in a radial orientation.

Other than some differences in the appearance and location of the second phase, the other changes produced by irradiation were similar in all the specimens from Capsule BMI-40-6. Densification of the UN occurred in the center of the pellets. This was particularly evident in Pellet 9A, which had a lower preirradiation density (see Figure 17). There were some indications of grain-boundary movement and possible grain growth. Small round gas bubbles appeared in the central region of the fuel, predominantly in the grain boundaries (Figures 19 and 21). The number of small bubbles or voids in the grain boundaries gradually decreased toward the pellet surface, and at about one-half the radius they were not observed in the grain boundaries. The microstructure in this region is shown in Figure 22.

A small zone in the cladding at the UN-cladding interface showed different etching behavior. The zone was about 6 μ thick and is shown in Figure 23. The layer may be nitrided stainless steel, although the recoil range of fission products is around 6 μ in iron. There did not appear to be any chemical reaction between the second phase and the cladding. The grain size of the stainless steel was quite large, with about three grains spanning across the 0.015-in.-thick cladding. This was probably produced during cladding by pressure bonding at 1150 C, since the maximum surface temperature during irradiation was estimated to be 615 C in the case of specimens from BMI-40-6. There appeared to be some carbide precipitation in the grain boundaries of the cladding. The bond between the stainless steel and UN was excellent; however, upon cooling after irradiation, the UN pulled away from the cladding, leaving an annular layer of UN about 0.005 to 0.015 in. thick attached to the cladding (Figures 17 and 18).

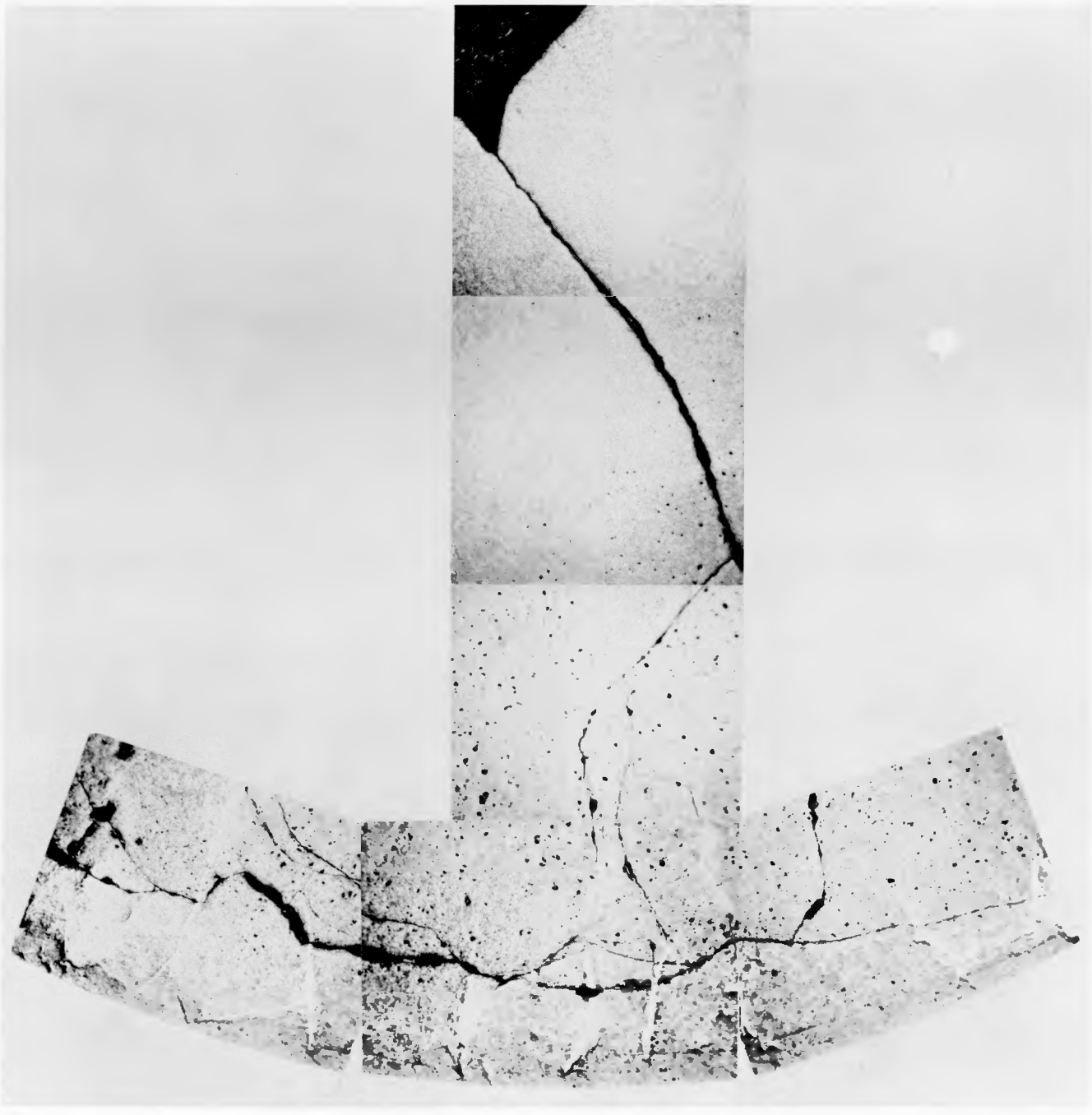

50X N98466

FIGURE 17. COMPOSITE VIEW OF UN PELLET 9A (MADE WITH WAX BINDER) FROM CAPSULE BMI-40-6 SHOWING A CROSS SECTION OF THE MICROSTRUCTURE FROM CENTER LINE (TOP) TO UN-STAINLESS STEEL CLADDING INTERFACE (BOTTOM)

The UN was irradiated to an uranium burnup of 3.8 a/o at a maximum center-line temperature of 1260 C and a maximum surface temperature of 615 C.

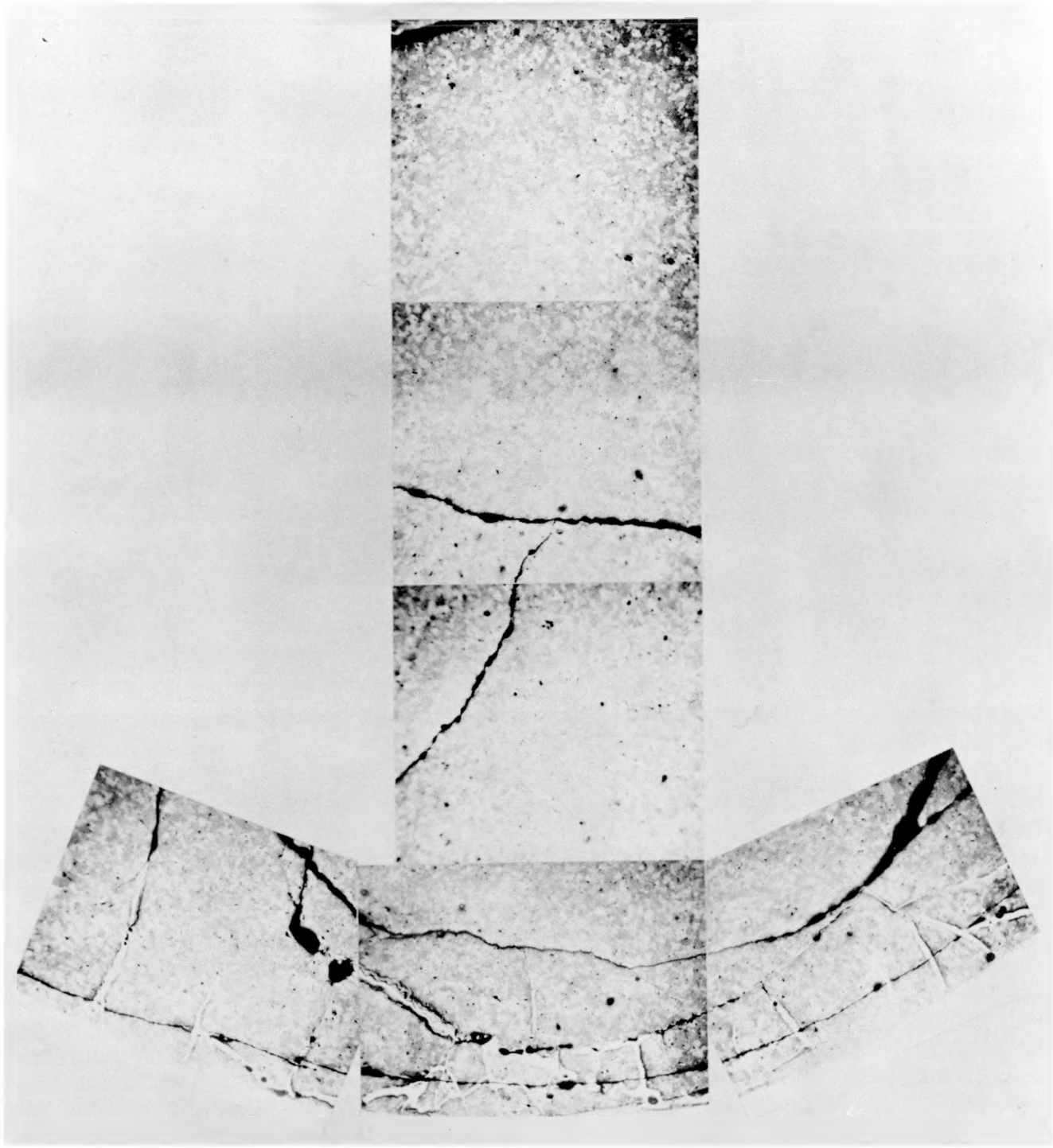

50X N98467

FIGURE 18. COMPOSITE VIEW OF UN PELLET 22 (NO BINDER) FROM CAPSULE BMI-40-6 SHOWING A CROSS SECTION OF THE MICROSTRUCTURE FROM CENTER LINE (TOP) TO UN-STAINLESS STEEL CLADDING INTERFACE (BOTTOM)

The pellet was irradiated under the same conditions as Pellet 9A shown in Figure 17.

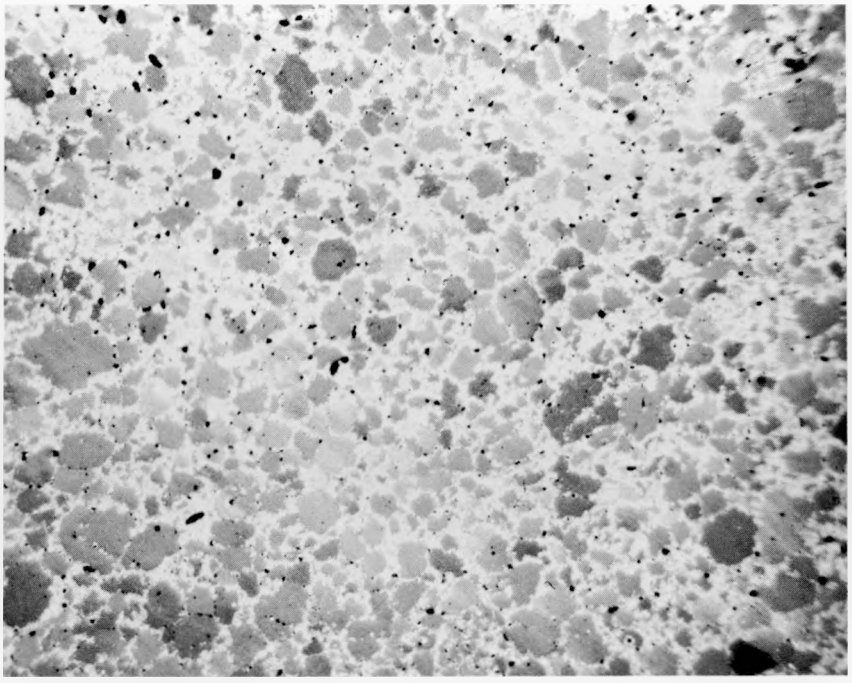

250X HC9443

FIGURE 19. MICROSTRUCTURE OF CENTER OF IRRADIATED UN PELLET 9A FROM CAPSULE BMI-40-6

Note the second phase and voids in grain boundaries.

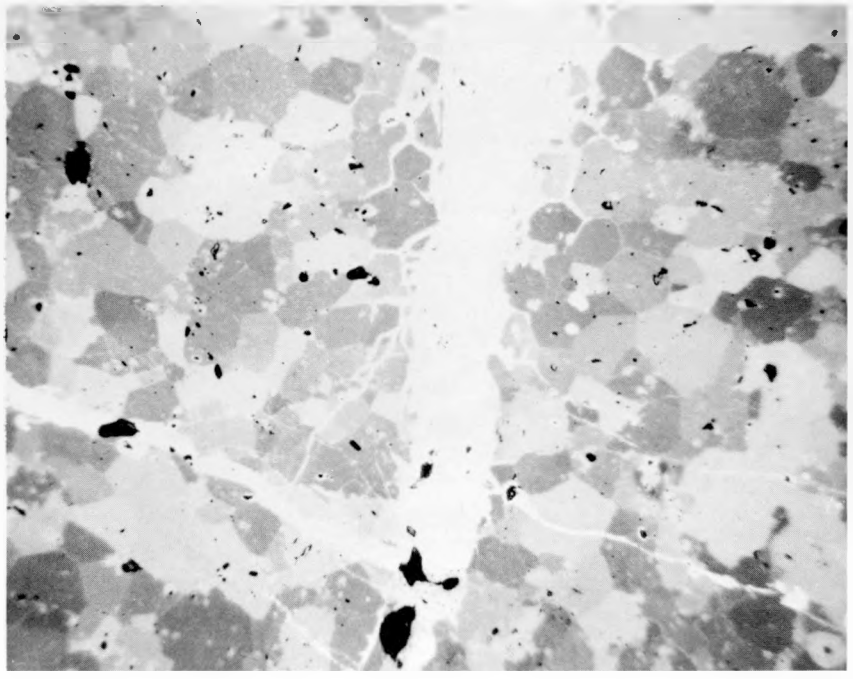

250X HC9402

FIGURE 20. MICROSTRUCTURE NEAR SURFACE OF IRRADIATED UN PELLET 22 FROM CAPSULE BMI-40-6 SHOWING APPEARANCE OF SECOND PHASE (WHITE)

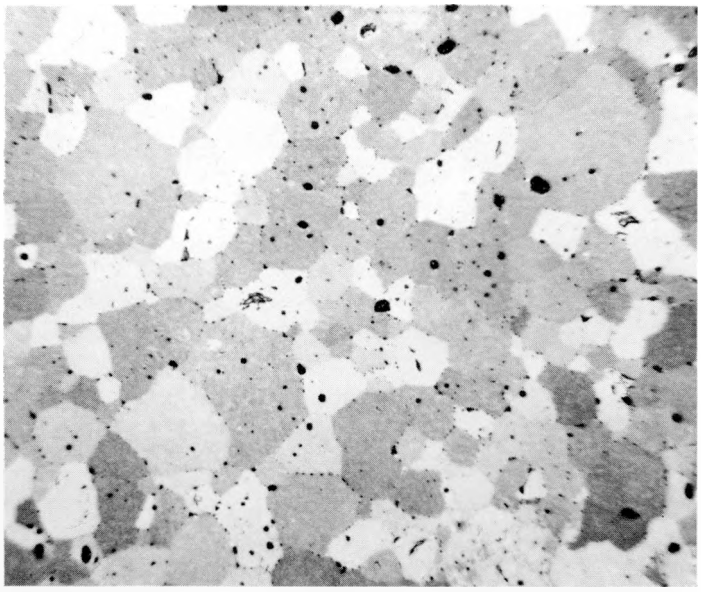

250X HC9403

FIGURE 21. CENTER OF IRRADIATED UN PELLET 22 FROM CAPSULE BMI-40-6

Note the small voids in the grain boundaries.

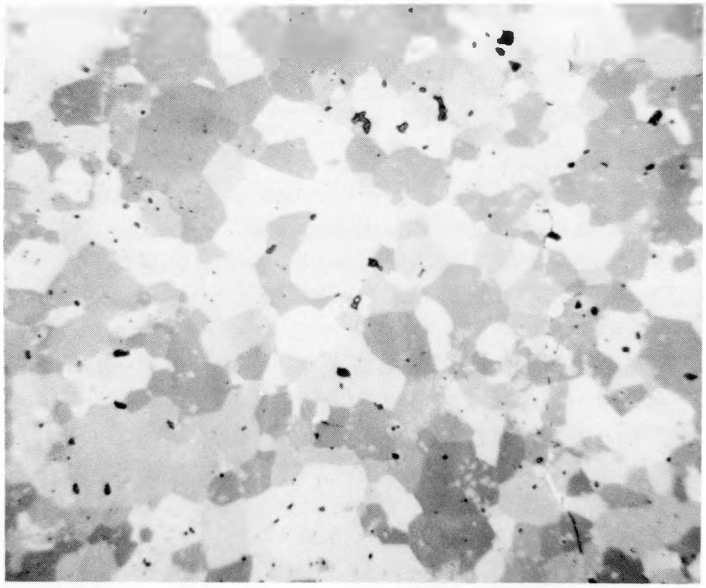

250X HC9858

FIGURE 22. THE MICROSTRUCTURE OF IRRADIATED UN PELLET 22 FROM CAPSULE BMI-40-6 AT A POINT MIDWAY BETWEEN CENTER AND EDGE OF THE PELLET

Note the absence of gas bubbles in the grain boundaries.

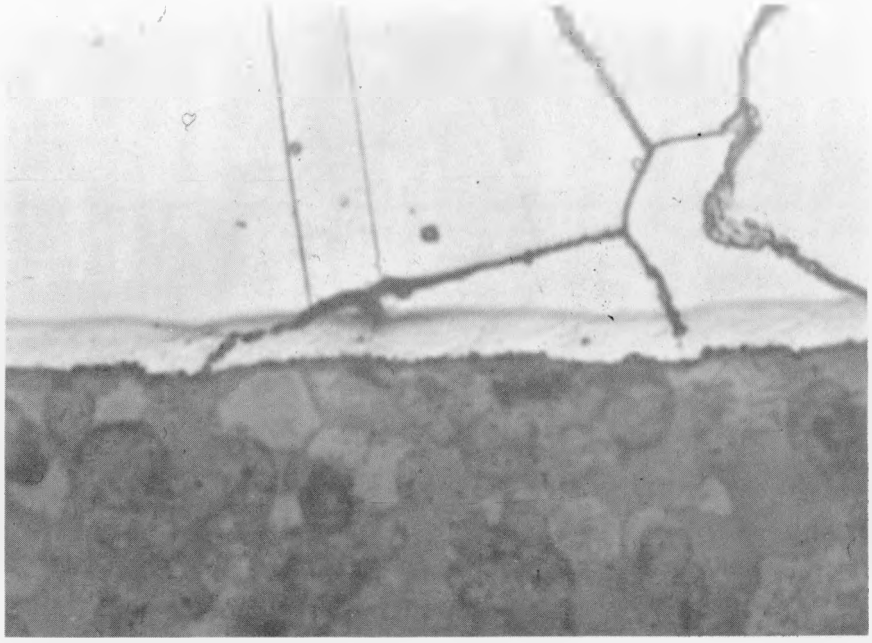

1000X HC9819

FIGURE 23. UN-TYPE 304 STAINLESS STEEL INTERFACE OF PELLET 9A FROM CAPSULE BMI-40-6

The maximum fuel-surface temperature was estimated to be 615 C.

Microhardness

Microhardness measurements were made on the specimens with the highest burnup. Knoop hardness measurements were made using a 50-g and a 200-g load. The average Knoop hardness from over 200 readings was 820 ± 150. Thus there was a general increase in the hardness of UN during irradiation, since the Knoop hardness of the unirradiated UN was 614 ± 16. Because of the spread in the postirradiation hardness measurements, differences in the hardness between the UN matrix and the second phase could not be detected. Microhardness measurements were also made on specimens subjected to lower burnups and irradiation temperatures. The average Knoop hardness was 800 ± 150, which was comparable to the hardness of the specimens irradiated to the higher burnups.

DISCUSSION OF RESULTS

The fracturing of the unclad UN during irradiation was probably due to a combination of thermal stresses created by the center line-to-surface temperature gradient and the presence of NaK. The fact that the center of the cylindrical fuel specimen was hotter than the surface produced axial compression in the center and axial tension on the surface. The axial tensile stress on the surface, if great enough, could produce the type of transverse fractures observed after irradiation. The temperature gradient necessary

to produce surface cracking (ΔT_f) has been calculated for UN and is around 44 C (using a transverse rupture strength of 10,000 psi, a Young's modulus of 33 x 10^6 psi[6], and a coefficient of thermal expansion of 9.7 x 10^{-6} per C[6]. Extensive cracking through the UN pellets would require larger temperature differences. In comparison, the ΔT_f for UC and UO_2 was calculated to be 44 C and 73 C, respectively. The transverse rupture strength of UN has not been measured, but it is likely to have a value similar to UC, which is around 10,000 psi at room temperatures.[7] The temperature gradients existing during the early part of the irradiation ranged from 50 to 645 C. The stresses necessary to produce fracture (or the ΔT_f) can be reduced if stress raisers, such as cracks, already exist on the surface. Two possible sources of cracks are microcracks remaining in the UN after powder-metallurgy fabrication and surface scratches produced by the grinding of the specimens to final dimensions. It is also possible that the presence of liquid metal (NaK) in contact with the surface of the UN could reduce the surface energy of the cracks and thus reduce the stress (or ΔT_f) needed to produce fracture. The presence of NaK is important since clad (slip-fitted) UN specimens subjected to center line-to-surface temperature differences of up to 370 C did not break up during irradiation, although they did show transverse fracture when subjected to slight mechanical shock after removal of the cladding.

Thermal stresses can also explain the fact that the fragment size of the fractured UN pellets decreased with increasing burnup and irradiation temperature. More specifically, the degree of breakup increased with increasing heat-generation rate. Since the thermal stress produced during irradiation is directly proportional to the heat-generation rate, the observed decrease in fragment size is what would be expected. This phenomenon has been observed in UO_2, where pellets were reduced to a fragment size which was stable to the thermal-gradient stresses produced during the initial cycles of thermal stressing.[8]

Although fracturing of the fuel occurred during irradiation, swelling of the UN was quite low. The percentage density decrease produced per 10^{20} fissions per cm^3 of fuel is shown as a function of irradiation temperature in Figure 24. This is a graphical representation of the data given in Tables 7 and 8. The temperature of the fuel gradually decreases during irradiation due to the significant burnup of the U^{235} atoms. This was particularly evident in Capsule BMI-40-6, where the initial fuel center-line temperature, $T_{c(i)}$, was 1260 C and the final fuel-surface temperature, $T_{s(f)}$, was 255 C. The range of temperatures the UN was irradiated at thus lie between the two extremes, $T_{c(i)}$ and $T_{s(f)}$, as shown in Figure 24. The dashed line represents the average fuel temperature for the irradiation, where the average irradiation temperature (T_A) at any time is given by $\left(\frac{T_c + T_s}{2}\right)$.

For UN irradiated below 250 C, the temperature spread during irradiation was quite small (<150 C), and the dashed curve (T_A) should represent the amount of swelling expected for a given irradiation temperature. For temperatures above 250 C, the swelling curve should be used with caution, keeping in mind the experimental conditions under which it was determined.

The swelling produced per unit of burnup was reduced considerably at irradiation temperatures above 250 C. This may be due to the annealing out of radiation-induced defects. Griffiths[9] has reported that quenched-in vacancies in UC anneal out around 700 C. The recovery of unit-cell size in irradiated UN has been observed to occur in three stages.[10] Approximately 30 per cent of the damage produced by neutron irradiation at 70 C anneals out around 150 C. Another 40 per cent recovers at temperatures

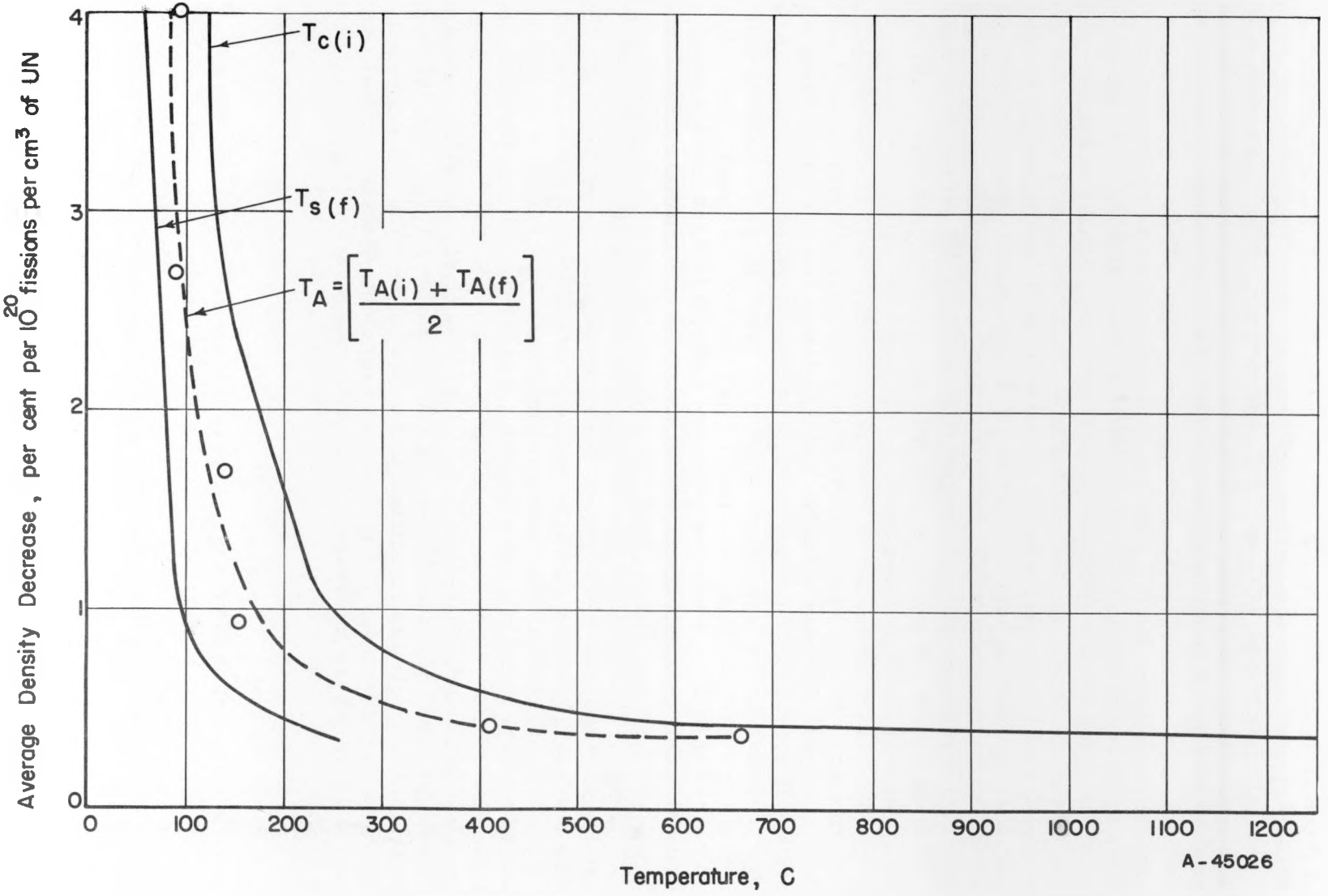

FIGURE 24. SWELLING OF UN AS A FUNCTION OF IRRADIATION TEMPERATURE

around 540 C. About 30 per cent of the radiation-induced unit-cell expansion remains in the UN above 640 C, indicating that a third recovery stage exists at higher temperatures.

The observed grain growth in the UN contained in Capsule BMI-40-6 can be attributed to the relatively high center-line temperature of 1260 C, and possibly the effects of fissioning and radiation. The general increase in size of all grains located near the axial center of the UN pellets seems to indicate that strain-free or nearly strain-free UN crystals grew continuously during the irradiation "heat treatment". Possible additional evidence of grain-boundary movement is provided by the gas bubbles that nucleated on the grain boundaries. Rows of bubbles were observed that apparently outlined the location of previous grain boundaries on which the gas bubbles had originally precipitated. It would be expected though that the gas bubbles would tend to prevent or hinder grain-boundary movement.

Uranium mononitride specimens in all of the capsules except BMI-40-6 were irradiated at temperatures less than 650 C. The diffusion coefficient for fission gases in UO_2 is very low and is considered temperature independent below 1000 C.[8,11] It seems reasonable to assume the same holds true for UN. That is, for irradiation temperatures less than 1000 C, the diffusion of fission gases through the UN lattice would be quite low. Preliminary data at Battelle for in-pile fission-gas release of UN suggest this assumption is valid.[12] The fission-gas atoms would most likely be retained in the UN lattice as supersaturated solutions. In the case of the UN with a center-line temperature of 1260 C (BMI-40-6), the fission-gas atoms are more mobile. This may permit them to diffuse to grain boundaries and precipitate as gas bubbles, since the grain boundaries would be a source of the vacancies needed to form gas bubbles. The observation that the number of gas bubbles gradually decreased from the center toward the outer surface of the pellet (i.e., with decreasing temperature) is consistent with this explanation. It should be pointed out that the center-line irradiation temperature was not above 1000 C over the entire irradiation (Table 7), and if it had been, the gas release might have been substantially higher.

The formation of these gas bubbles on the grain boundaries during irradiation may affect the gas retention and mechanical properties of UN. The low fission-gas release (0.3 to 0.6 per cent) is related to the retention of the fission-gas atoms in the UN lattice. The nucleation and diffusion of fission-gas bubbles at the grain boundaries may lead to high gas release. Also, gas bubbles at the grain boundaries could lead to grain-boundary separation, grain-boundary creep, etc., that would reduce the mechanical strength of UN and lead to enhanced swelling.

Hydrogen produced by the $N^{14}(n,p)C^{14}$ reaction does not appear to be a problem in UN. No solubility of hydrogen (<1 ppm) in UN has been observed after the UN was equilibrated with hydrogen at 1 atm at 500 C for 65 hr and at 800 C for 24 hr.[1] It is expected that the hydrogen would diffuse out of the UN, as the gas-release data seem to indicate. The role of hydrogen in the gas-bubble formation is not known. The presence of hydrogen in the UN did not drastically affect the dimensional stability of the fuel. If there were any effects, they would be expected to show up in the low-enrichment specimens, where the ratio of the amount of hydrogen formed to the amount of fission gas formed was the largest. The dimensional and density measurements did not indicate any marked swelling of the low-enrichment specimens (Capsules BMI-40-1 and BMI-40-2, Table 8) even though these specimens were irradiated at the lowest temperatures and would thus show less recovery of the radiation-induced damage.

In the pre- and postirradiation metallography, a second phase was observed. Prior to irradiation it was uniformly distributed. In samples prepared with a wax binder, it existed in greater amounts and was associated with pores. Recent studies[1] have indicated that this second phase is composed of UO_2 and a higher nitride (most probably $UN_{1.5+x}$). The postirradiation metallography indicated that the location and appearance of this second phase does not change significantly at irradiation temperatures below 650 C (Capsules BMI-40-1 through BMI-40-5). However, for an irradiation center-line temperature of 1260 C, the second phase relocated predominantly near the fuel surface. The diffusion of nitrogen under a thermal gradient could produce a higher uranium nitride in the cooler region of the fuel.

CONCLUSIONS

The aim of this study was to help establish the feasibility of uranium mononitride as a reactor fuel material by investigating its radiation resistance. It is concluded that UN has good irradiation stability under the conditions tested and warrants further study. This conclusion is based on the following observations:

(1) No marked dimensional instability was observed in the UN irradiated at initial surface and center-line temperatures as high as 615 and 1260 C, respectively, and to total uranium burnups as high as 3.8 a/o.

(2) The amount of fission gas released by UN was only 0.3 to 0.6 per cent of that produced in the fuel.

(3) Hydrogen produced by the $N^{14}(n,p)C^{14}$ reaction did not appear detrimental to the radiation stability of UN.

(4) Uranium mononitride was compatible with Type 304 stainless steel at fuel-surface temperatures up to 615 C.

(5) No chemical reaction occurred between uranium mononitride and NaK during irradiation.

REFERENCES

(1) Speidel, E. O., and Keller, D. L., "Fabrication and Properties of Uranium Mononitride", BMI-1633 (May 30, 1963).

(2) Lyon, R. N., Ed., Liquid-Metals Handbook, 2nd Ed., Report NAVEXOS-P-733 (Rev.), USAEC, U. S. Navy, U. S. Government Printing Office, Washington, D. C., June, 1950 (Revised 1954).

(3) "The P-3 Program for the IBM Computer", DC-56-7-30 (May 31, 1956).

(4) Tipton, C. R., Ed., Reactor Handbook, Vol. 1, Materials, Interscience Publishers, Inc., New York (1960).

(5) Musser, W., Bugl, J., and Bauer, A. A., "Metallography of Uranium-Nitrogen Compounds", Presented at the 17th Meeting of the AEC Metallography Group, May, 1963, Los Alamos Scientific Laboratory.

(6) Keller, D. L., "Development of Uranium Mononitride", Quarterly Progress Report for July-September, 1961, to Joint U.S.-Euratom Research and Development Board, EUR/AEC-169 (October 1, 1961).

(7) Rough, F. A., and Chubb, W., "Progress on the Development of Uranium Carbide-Type Fuels", BMI-1370 (August 21, 1959).

(8) Belle, J., Ed., Uranium Dioxide: Properties and Nuclear Applications, Naval Reactors, Division of Reactor Development, USAEC (July, 1961), p 635.

(9) Griffiths, L. B., "Quenching Vacancies in Uranium Monocarbide", Phil., Mag., 7, 827 (May, 1962).

(10) Rogers, M. D., and Adam, J., "Radiation Damage and Its Thermal Recovery in Uranium Monocarbide and Uranium Mononitride", AERE-R-4046 (June, 1962).

(11) Melehan, J. B., Barnes, R. H., Gates, J. E., and Rough, F. A., "Release of Fission Gases From UO_2 During and After Irradiation", BMI-1623 (March 26, 1963).

(12) Dayton, R. W., and Dickerson, R. F., "Progress Relating to Civilian Applications During April, 1963", BMI-1630 (May 1, 1963).

RAW/JFL/JB/JEG:pa